Field Crops Research 304 (2023) 109168

Contents lists available at ScienceDirect

Field Crops Research

journal homepage: www.elsevier.com/locate/fcr

Unveiling the phenotypic landscape of stalk lodging resistance in diverse maize hybrids

Bharath Kunduru [a], Rohit Kumar [a], Manwinder S. Brar [a], Christopher J. Stubbs [b], Kaitlin Tabaracci [c], Norbert T. Bokros [d], William C. Bridges [e], Douglas D. Cook [f], Seth DeBolt [d], Christopher S. McMahan [e], Daniel J. Robertson [c], Rajandeep S. Sekhon [a,*]

[a] Department of Genetics and Biochemistry, Clemson University, Clemson, SC 29634, USA
[b] School of Computer Sciences and Engineering, Fairleigh Dickinson University, Teaneck, NJ 07666, USA
[c] Department of Mechanical Engineering, University of Idaho, Moscow, ID 83844, USA
[d] Department of Horticulture, University of Kentucky, Lexington, KY 40546, USA
[e] School of Mathematics and Statistical Sciences, Clemson University, Clemson, SC 29634, USA
[f] Department of Mechanical Engineering, Brigham Young University, UT 84602, USA

ARTICLE INFO

Keywords:
Maize
Stalk
Lodging
Phenotype
Modulus
Moment of inertia

ABSTRACT

Context: Stalk lodging causes up to 43 % of yield losses in maize (*Zea mays* L.) worldwide, significantly worsening food and feed shortages. Stalk lodging resistance is a complex trait specified by several structural, material, and geometric phenotypes. However, the identity, relative contribution, and genetic tractability of these intermediate phenotypes remain unknown.

Objective: The study is designed to identify and evaluate plant-, organ-, and tissue-level intermediate phenotypes associated with stalk lodging resistance following standardized phenotyping protocols and to understand the variation and genetic tractability of these intermediate phenotypes.

Methods: We examined 16 diverse maize hybrids in two environments to identify and evaluate intermediate phenotypes associated with stalk flexural stiffness, a reliable indicator of stalk lodging resistance, at physiological maturity. Engineering-informed and machine learning models were employed to understand relationships among intermediate phenotypes and stalk flexural stiffness.

Results: Stalk flexural stiffness showed significant genetic variation and high heritability (0.64) in the evaluated hybrids. Significant genetic variation and comparable heritability for the cross-sectional moment of inertia and Young's modulus indicated that geometric and material properties are under tight genetic control and play a combinatorial role in determining stalk lodging resistance. Among the twelve internode-level traits measured on the bottom and the ear internode, most traits exhibited significant genetic variation among hybrids, moderate to high heritability, and considerable effect of genotype × environment interaction. The marginal statistical model based on structural engineering beam theory revealed that 74–80 % of the phenotypic variation for flexural stiffness was explained by accounting for the major diameter, minor diameter, and rind thickness of the stalks. The machine learning model explained a relatively modest proportion (58–62 %) of the variation for flexural stiffness.

Conclusions: Characterization of stalk and internode properties using standard phenotyping methods revealed tremendous variation for intermediate phenotypes underlying stalk lodging resistance. The intermediate phenotypes showed moderate to high heritability, indicating their genetic tractability for improving stalk lodging resistance. Stalk geometric and material properties showed complementarity in determining stalk flexural stiffness. Engineering-informed models outperformed machine learning approaches in explaining variation for flexural stiffness.

Implications: Identification of genetically tractable intermediate phenotypes will boost efforts toward genetic improvement of stalk lodging resistance in maize. Discovering the genetic architecture of the intermediate traits will enhance our understanding of the biological underpinning of stalk lodging resistance.

* Correspondence to: Department of Genetics and Biochemistry, Clemson University, 105 Collings Street, 314 Biosystems Research Complex, Clemson, SC 29634, USA.
E-mail address: sekhon@clemson.edu (R.S. Sekhon).

https://doi.org/10.1016/j.fcr.2023.109168
Received 12 May 2023; Received in revised form 11 October 2023; Accepted 16 October 2023
Available online 29 October 2023

1. Introduction

Plant lodging, a permanent rotational displacement of plants from their natural erect habit, severely undermines the yield and quality of crops and limits global food and nutritional security. Cereal crops, which account for 32 % of the worldwide food and feed supply, can experience yield losses of up to 80 % due to lodging (FAO, 2022; Foulkes et al., 2010; Rajkumara, 2008). In maize (*Zea mays* L.), one of the major cereal crops, a survey of various reports revealed that lodging causes 2–43 % of yield losses annually (Carter and Hudelson, 1988; Flint-Garcia et al., 2003; Lindsey et al., 2021). Considering even the lowest reported yield loss (2 %) and the global export price of maize in 2020–21 (FAO, 2022; USDA, 2021), these losses translate into an estimated annual global loss of at least 6 billion US dollars. Given that maize and other cereal crops are increasingly sought for various industrial applications besides food and feed, the economic impact of lodging is expected to increase significantly in the future. In the past half-century, considerable genetic improvement of lodging resistance in maize has been achieved through conventional breeding for various traits related to stalk strength and transgenic approaches targeting resistance to insects (Martin et al., 2004; Niu et al., 2022; Thompson and Narva, 2009). However, the adoption of intensive agricultural practices, including higher planting densities and increased fertilizer application, has escalated lodging incidence (Rajkumara, 2008; Shah et al., 2021). Lodging is also highly influenced by weather events, mainly wind velocity and rainfall, and the increasingly variable and extreme global climate will further aggravate lodging incidence and related economic losses (Carter and Hudelson, 1988; Zheng et al., 2023). Lodging is expected to exacerbate economic losses, especially in developing countries whose economies depend heavily on agriculture.

There are two types of lodging observed in maize plants: root lodging, caused by the inability of the root to keep the plant fully anchored to the soil, and stalk lodging, caused by the mechanical failure of the stem. Plants are more susceptible to root lodging during vegetative stages when the root system is not fully developed, and consequently, windy and rainfall conditions early in the growing season lead to a greater incidence of root lodging (Carter and Hudelson, 1988). Yield losses due to root lodging depend upon the stage of crop growth and usually become higher as the crop reaches physiological maturity (Lindsey et al., 2021). Stalk lodging can be further broken down into two distinct types. If the stalk failure occurs before flowering, it is termed greensnap, whereas if the stalk breaks after physiological maturity, it is termed late-season stalk lodging or simply stalk lodging (Cook et al., 2019; Erndwein et al., 2020). While both types of failure produce the same outcome (i.e., failure of the stalk), they are distinct phenomena governed by separate and unique environmental and physiological conditions. For instance, turgor pressure and leaf sheath strength are more important factors for greensnap, while secondary cell wall differentiation and lignification play a larger role in late-season stalk lodging (Elmore and Ferguson, 1999; Manga-Robles et al., 2021). Both greensnap and late-season stalk lodging can cause complete yield losses due to mechanical damage to the vascular tissues (Albrecht et al., 1986; Khobra et al., 2019). This study is focused on the problem of late-season stalk lodging, which will be referred to simply as *stalk lodging* throughout the manuscript. Given the severe impact of stalk failure on crop production, a comprehensive understanding of the genetic architecture of stalk lodging resistance is critical for preventing yield and the associated economic losses.

Stalk lodging resistance is a complex trait influenced by several external factors, including crop management practices, pest and disease pressure, and weather patterns (Loesch Jr. et al., 1962; Xue et al., 2020; Ye et al., 2016). Several internal factors also influence stalk lodging resistance, including structural, material, and geometric properties of the stalk that are determined by the plant genotype (Erndwein et al., 2020; Robertson et al., 2022; Robertson et al., 2017; Seegmiller et al., 2020; Stubbs et al., 2020a, 2020b, 2022b). Multiple interactions between these internal and external factors exist at various temporal and spatial scales, producing a highly complex plastic phenotype that is challenging to evaluate in genetic and breeding studies (Stubbs et al., 2023). In particular, the lack of affordable, reliable and reproducible methods for measuring stalk lodging resistance in field conditions has been a major obstacle in resolving the genetic architecture of this trait. These impediments have prompted the use of various intermediate phenotypes, including breaking strength, crushing strength, and rind penetrance resistance, as proxies for stalk lodging resistance in genetic studies (Durrell, 1925; Zuber and Grogan, 1961). However, the mechanical tests used to acquire these intermediate phenotypes produce failure types and patterns inconsistent with natural stalk lodging patterns (Robertson et al., 2015). Other approaches have relied on exposing the plants to high-velocity winds via low-flying helicopters or artificial wind machines to select genotypes with stronger stalks (Barreiro et al., 2008; Bayer, 2022). However, this approach suffers from several drawbacks, including unnatural wind loading inconsistent with that experienced by the stalks in nature and bulky and expensive equipment needed to collect such phenotypes. Because of these challenges, counting the percentage of lodged stalks at harvest is still one of the most common methods of assessing lodging resistance. This method is likewise fraught with challenges as it is completely reliant on weather conditions, which vary from year to year. For example, under optimal growing environments, little to no lodging is observed thus exaggerating lodging resistance and making it impossible to rank the relative lodging resistance of different genotypes. Conversely, extreme weather (e.g., hurricanes) may cause all the genotypes in a study to lodge thus underestimating lodging resistance and again eliminating the ability of

Box 1 – Description of key terms

Stalk flexural stiffness (***a.k.a. stalk flexural rigidity***) – A measure of the ability of a stalk to resist bending deformation such that higher flexural stiffness indicates a higher magnitude of the force required to bend a stalk to a certain distance.

Stalk lodging resistance – A conceptual, holistic assessment of the ability of a genotype to withstand external forces, including wind and gravity, and biotic factors, including insect pests and diseases that contribute to stalk lodging.

Lodging incidence – A count or proportion of plants lodged in a defined area.

Geometric property – The property of an object derived from its geometric form, including size, shape, length, thickness, curvature, etc.

Material property – Intrinsic properties that determine the response of a material to physical loads. These properties are determined by molecular structure and composition and are independent of the stalk geometry.

Structural property – Characteristics of a structure that affect its mechanical response to physical loads and are the resultant combination of geometric and material properties.

researchers to quantify the relative lodging resistance of genotypes in the study. Therefore, using natural lodging counts to assess lodging resistance requires growing plants in multiple locations over multiple years to obtain an estimated ranking of relative lodging resistance.

To overcome the hindrances posed by the existing phenotyping methods, a field-based phenotyping platform, Device for Assessing Resistance to Lodging IN Grains (DARLING), was developed to obtain estimates of stalk flexural stiffness of field-grown plants by replicating the mechanical loads and stress patterns experienced by naturally lodged plants (Cook et al., 2019). We have recently shown that stalk flexural stiffness and bending strength estimates generated by DARLING are significant predictors of natural stalk lodging incidence (Robertson et al., 2016; Sekhon et al., 2020; Stubbs et al., 2020c). For example, we have shown that stalk bending strength measurements of 47 maize hybrids gathered in 3 locations were predictive of the natural lodging incidence rates of those same 47 maize hybrids collected in 98 distinct environments (Sekhon et al., 2020). The availability of this new phenotyping method provides opportunities to identify phenotypic and genetic determinants of stalk lodging resistance in maize on reduced time scales as compared to conducting very large multi-year and multi-environment studies of natural lodging incidence.

Our previous studies, based on structural engineering beam theory tenets, have shown that stalk flexural stiffness measured by the DARLING can explain 81 % of the variation in stalk bending strength (Robertson et al., 2016). A structural engineering beam model of flexural stiffness (FS) is given by $FS = EI$, where E denotes Young's modulus, a representation of the stalk material properties, and I indicates the cross-sectional moment of inertia, hereafter referred to simply as *moment of inertia in* the manuscript, a summary of the geometric properties (Cook et al., 2019; Robertson et al., 2017; Stubbs et al., 2022b). The moment of inertia is a geometric property derived from stalk diameter and rind thickness that describes the cross-sectional organization of the stalk biomass relative to the centroidal axis of the stalk. Young's modulus is a material property used to describe the inherent stiffness of a material (i.e., resistance to deformation in the presence of externally applied loads). The relative contribution of Young's modulus and the moment of inertia to stalk flexural stiffness and stalk lodging remains to be fully understood. The underlying genetic architecture of these important traits is likewise unknown.

The structural properties of individual internodes along the length of the stalk influence the overall structural behavior of the stalk (i.e., the stalk flexural stiffness and stalk bending strength). The effect of structural, geometric, and material properties of individual internodes on stalk lodging has been investigated in earlier studies, which generated some valuable insights into their variable impact on stalk lodging (Xie et al., 2022; Zhan et al., 2022). Phenotyping of individual internodes could aid in dissecting organ and sub-organ level phenotypic determinates of stalk lodging. However, variation in internode number, both within and across genotypes, poses significant challenges to statistical tests used to determine the effect of individual internodes on stalk lodging. Identifying analytical approaches for teasing apart the impact of individual internodes is essential to generating a comprehensive understanding of stalk lodging resistance.

In this study, we set out to 1) standardize phenotyping protocols to systematically measure a diverse set of intermediate phenotypes related to late-season stalk lodging, 2) understand the phenotypic variation and the role of genotype × environment (G×E) interaction in specifying these intermediate phenotypes, 3) identify the relevance of material and geometric proprieties represented by Young's modulus and moment of inertia in the determination of stalk flexural stiffness, and 4) employ engineering-informed and machine learning modeling to decipher the relationship between intermediate phenotypes and stalk lodging resistance. Our findings will elucidate the relationship between intermediate phenotypes and stalk strength, help identify the genetic determinants of the intermediate phenotypes, and boost breeding efforts to improve the climate resilience of maize and related grasses.

2. Materials and methods

2.1. Plant material and experimental details

We generated 16 maize hybrids by crossing B73 and Mo17 inbred lines belonging to stiff stalk and non-stiff stalk heterotic groups, respectively, to 8 genetically diverse inbred lines (Table 1) (Hirsch et al., 2014; White et al., 2020). The hybrids were evaluated at the Clemson University Calhoun Field Laboratory, South Carolina, United States (34°40'N, 82°50'W) during the summer of 2019 and 2021. The two years represent two unique environments with distinct growing conditions, as indicated by the meteorological data (Fig. 1). The experimental field is characterized by sandy loam Toccoa soil with a pH of 6.0, and moisture levels generally remain at field capacity due to the vicinity of the field location to Lake Hartwell. The experiment was laid out in a randomized complete block design with two replications in both environments. The hybrids were planted in two-row plots with a 6.1 m row length and 0.76 m row-to-row distance, resulting in a 9.272 m^2 plot area and a target planting density of 70,000 plants ha^{-1}. To supplement the soil nutrients, 57 kg ha^{-1} of nitrogen, 106 kg ha^{-1} of phosphorus, and 93 kg ha^{-1} of potassium were applied during land preparation, and an additional 85 kg ha^{-1} of nitrogen was applied at the V8 stage. Recommended agronomic practices were followed throughout the growing season to prevent weed, insect, and disease infestations in the experimental plots.

2.2. Stalk sampling and data recording

In each plot, 40 representative plants were selected and labeled to maintain the individual plant identity, and data were recorded on flowering, plant height, and ear height. Further, stalk flexural stiffness

Table 1
Details of the inbred parents and resulting hybrids used in the study.

#	Parent	Male/Female	Heterotic group	Year of release	Growing Degree Units[$]	Resulting hybrids	
						B73	Mo17
1	B73	Male	stiff-stalk	1972	1396–1716	-	-
2	Mo17	Male	non-stiff-stalk	1964	1443–1645	-	-
3	CH701–30	Female	stiff-stalk	1984[#]	1396–1429	CH701–30/B73	CH701–30/Mo17
4	MoG	Female	unknown	1945[#]	1672–2102	MoG/B73	MoG/Mo17
5	PHPR5	Female	stiff-stalk	1992	1440	PHPR5/B73	PHPR5/Mo17
6	A680	Female	stiff-stalk	1987	1396–1681	A680/B73	A680/Mo17
7	N7A	Female	stiff-stalk	1969	1556–1728	N7A/B73	N7A/Mo17
8	Mo45	Female	unknown	1994	1443–1794	Mo45/B73	Mo45/Mo17
9	PHZ51	Female	non-stiff-stalk	1986	1396–1455	PHZ51/B73	PHZ51/Mo17
10	PHG35	Female	non-stiff-stalk	1983	1467–1700	PHG35/B73	PHG35/Mo17

#, These inbred lines were released in or before the year mentioned in the table. $, Growing degree units included in the table are measured in degrees Fahrenheit from planting to 50 % silking (https://www.ars-grin.gov/).

was tested by pushing the stalks 38–42 days after flowering using DARLING (Cook et al., 2019; Sekhon et al., 2020). Before testing, leaves, sheaths, cobs, and the stalk section above the primary ear-bearing node were removed. The stalks were prepared this way to increase the accuracy of the obtained force and displacement data, and the prepared stalks were tested immediately to prevent moisture loss. In each row, the ear height of the shortest stalk was used to determine the test height for DARLING, and the same test height was used for evaluating all plants in that row. After testing, the stalks were collected from the field by cutting them at ground level. The collected stalks were dried for six weeks under controlled conditions (38 °C and at 35 % RH) and stored at room temperature for recording data on the intermediate phenotypes.

The approach used for recording various intermediate phenotypes is described in Table 2. For metabolic analysis, we separately examined the internode immediately below the primary ear-bearing node, designated as the ear internode, and the lower-most elongated internode, referred to as the bottom internode (Fig. 2). These two internodes were excised from six randomly chosen stalks from each plot, ground in a Retsch SM 300 cutting mill at 1700 rpm, sifted using a 2 mm sieve, and further ground with a pestle and mortar to increase the particle fineness. The ground tissues thus obtained from each plot constituted a biological replicate, and we generated two such replicates for each hybrid. Metabolic data on cellulose, hemicellulose, and lignin contents in the ear and bottom internodes was generated by Dairyland Laboratories, Inc. (Arcadia, WI) using our published approach (Sekhon et al., 2020).

Only healthy, representative, and uniform stalks were used in our analyses. Since the data collection was done in multiple stages in both field and lab, we ensured that, for a given stalk, data on most, if not all, traits were available. Stalks with missing data in multiple traits were discarded. These quality control measures resulted in variation in the actual sample size for the number of stalks analyzed for each hybrid. In 2019, we evaluated 650 stalks corresponding to the 16 maize hybrids with a mean and median of 41 and 42 stalks per hybrid, respectively. In 2021, we assessed 571 stalks with a mean and median of 36 and 40 per hybrid, respectively. In terms of sample size, the number of stalks evaluated for each hybrid varied from 16 to 54 and 16 to 53 in 2019 and 2021, respectively (Supplementary Table B1). Although the plant stand in the plots was fairly uniform, we followed strict quality measures during phenotyping and only sampled healthy, representative, and uniform-looking plants. Furthermore, since the data collection was done in multiple stages in the field and the lab, stalks with missing data on one or more traits were discarded. These quality control measures resulted in variation in the number of stalks analyzed for each hybrid.

2.3. Imputation of missing phenotypic data

The relatedness among the intermediate phenotypes was used for data imputation using the factorial analysis for the mixed data approach implemented using the *imputeFAMD* function in the *missMDA* R package separately for each environment (Josse and Husson, 2016). The *imputeFAMD* analysis was based on six principal components. The number of elongated internodes on the stalk below the primary ear-bearing node, hereafter referred to as the *number of internodes*, showed wide variation within and among hybrids. Out of 1221 stalks evaluated, only 193 (15.81 %) and 29 (2.38 %) stalks had 7th and 8th internodes, respectively (Supplementary Fig. A1). Therefore, due to insufficient data on these two internodes, only the data from the bottom six internodes was used for imputations and further analyses. The internodes were labelled bottom-up, starting from the bottom internode (e.g., the bottom internode, which is the first internode as per this convention, was designated as IN1).

2.4. Weighted approach to project internode phenotypes to stalk sections

There was a variable number of internodes within and across hybrids, which posed a challenge for internode-wise comparison of phenotypes. To circumvent this problem, we systematically aggregated the phenotype data collected on individual internodes of each stalk into three distinct sections designated as top, middle, and bottom (Fig. 3). These sections were defined by evenly dividing the stalk of the plant into three discrete regions, spanning from the ground level to the test height specified for the DARLING phenotyping (Section 2.2). The intermediate phenotypes for these three sections were determined as the weighted average of the corresponding phenotypes measured on the internodes, where the weights were set based on the size of the overlap between the individual internodes and the stalk sections. The data obtained through this approach was used to conduct the engineering-informed and machine learning analyses outlined in Sections 2.6 and 2.7.

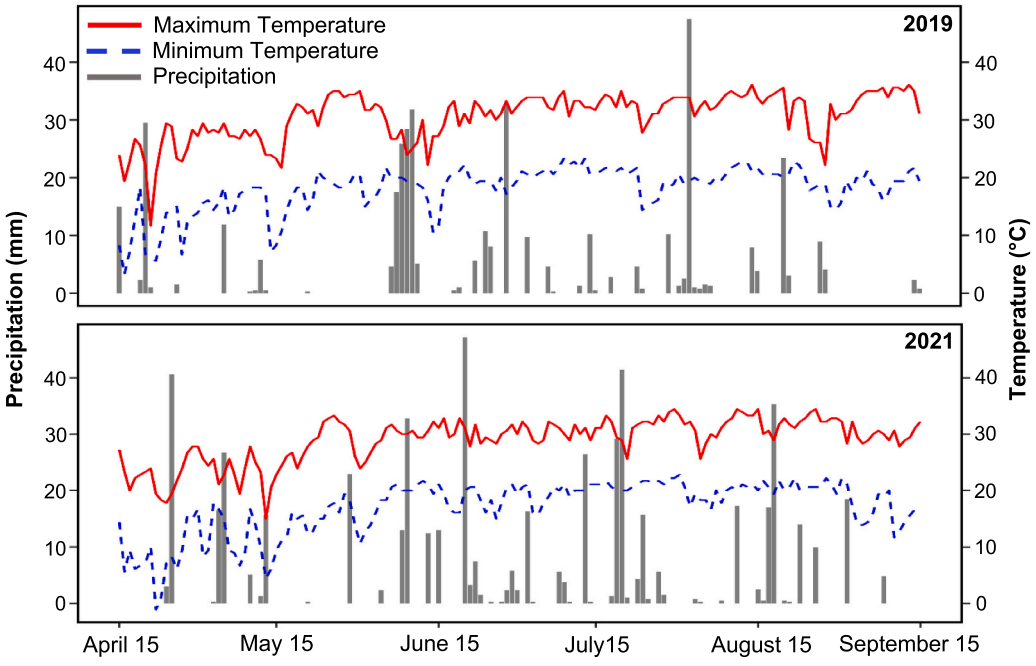

Fig. 1. Daily weather data during the growing seasons in 2019 and 2021.

Table 2
Protocols for different intermediate phenotypes measured.

#	Phenotype	Category	Sampling unit	Phenotyping Protocol	Source
1	Plant height	Geometric	Stalk	The linear distance between the soil surface and the tip of the central spike of the tassel is measured with a measuring stick.	(Stubbs et al., 2023)
2	Ear height	Geometric	Stalk	The linear distance between the soil surface and the primary ear-bearing node is measured with a measuring stick.	(Stubbs et al., 2023)
3	Number of internodes	Geometric	Stalk	The number of elongated internodes between the primary ear-bearing node and the soil surface is counted visually. Note that, if the goal is to count all internodes (elongated and compressed), the number of leaves (both juvenile and adult) should be used.	
4	Flexural stiffness	Structural	Stalk	Prepared stalks are loaded with an incremental force with DARLING until the stalk is deflected but not broken or buckled. The reading is discarded if root lodging is observed.	(Cook et al., 2019; DeKold and Robertson, 2023)
5	Rind puncture resistance	Structural	Internode	The internode is punctured using an Instron universal testing system, and the rind puncture resistance is recorded as the peak force obtained from the force-displacement graph (see Fig. 2).	(Seegmiller et al., 2020)
6	Major diameter	Geometric	Internode	The largest possible diameter of an internode is measured in the direction perpendicular to the plane of the groove of the ear (if present) or to the point of leaf attachment at the basal node of the internode and measured using a Vernier caliper.	
7	Minor diameter	Geometric	Internode	The smallest possible diameter of an internode is measured in the direction of the plane of the groove of the ear (if present), or to the point of leaf attachment at the basal node of the internode using an Instron or a Vernier caliper. While using the Instron, the displacement of the Instron probe between the entry and exit points of the stalk tissues corresponds to the minor diameter of the internode (see Fig. 2).	(Seegmiller et al., 2020)
8	Rind thickness	Geometric	Internode	Displacement of the Instron probe from the epidermis to the pith of the stalk as measured from the force-displacement graph (see Fig. 2).	(Seegmiller et al., 2020)
9	Moment of inertia	Geometric	Stalk and internode	Calculated using the major diameter, minor diameter, and rind thickness using the formula: I= π[qp3 – (q – 2r)(p – 2r)3]/64, where I denotes the moment of inertia, p and q represent major and minor diameter, respectively, and r indicates rind thickness.	
10	Section modulus	Geometric	Internode	Calculated using the major diameter, minor diameter, and rind thickness using the formula: Section modulus = Moment of inertia/(minor diameter/2)	(Robertson et al., 2017)
11	Internode length	Geometric	Internode	The length of the stalk segment between two successive nodes as measured using a measuring stick.	
12	Integrated puncture score	Structural	Internode	Derived from the force-displacement graph of stalk puncture tests as described in Stubbs et al. (2020a).	(Stubbs et al., 2020a)
13	Young's modulus	Material	Stalk	Calculated as the quotient of flexural stiffness (F) by the moment of inertia (I) such that Young's modulus (E) = F/I	
14	Linear density	Geometric and Material	Internode	Individual internodes are separated by cutting the stalks 1 cm inwards from the ridge of each node. These internode sections are weighed and measured for their length. The linear density is obtained by dividing weight by length.	

2.5. Structural engineering-informed modeling to predict stalk flexural stiffness

To summarize geometric phenotypes for distinct sections (top, middle, and bottom) of the stalk, we considered a weighted combination of the three intermediate phenotypes, including rind thickness (x_{ij1}), major diameter (x_{ij2}), and minor diameter (x_{ij3}), where j denotes the internode on which the phenotype was measured, with j = 1 being the bottom, j = 2 being the middle, and j = 3 being the top section of the stalks. The weighted combinations for each phenotype were computed as:

$$x_{ik} = \left(\sum_{j=1}^{3} w_j x_{ijk}\right) \Big/ \left(\sum_{j=1}^{3} w_j\right).$$

To identify the "optimal" weighting scheme, we considered every $(w_1, w_2, w_3) \in \Omega = [(\omega_1, \omega_2, \omega_3) : \omega_1 = 0, 0.1, \ldots, 1; \omega_2 = 0, 0.1, \ldots, 1; \omega_3 = 0, 0.1, \ldots, 1]$. Once the weighted averages were computed, we computed the moment of inertia of the plant as:

$$I_i = \pi[x_{i3}x_{i2}^3 - (x_{i3} - 2x_{i1})(x_{i2} - 2x_{i1})^3]/64.$$

A regression model was fit of the following form:

$$FS_i = \beta_0 + \sum_{h=1}^{16} \alpha_h I_i H_{ih} + \epsilon_i,$$

In this model, β_0 is an intercept term, α_h is a slope parameter, H_{ih} is a dummy variable that encodes the hybrid type (i.e., $H_{ih} = 1$ if the ith plant is of the hth hybrid type and $H_{ih} = 0$ otherwise), and ϵ_i is the random error. A few comments are warranted. First, the form of the regression model is directly inspired by the structural engineering beam theory that describes the strength of the stalk. Second, the slope parameters take the place of Young's modulus, and through the interaction model, we allowed Young's modulus to vary across the hybrid types. This approach will enable us to directly estimate Young's modulus, a trait that cannot be readily phenotyped. Moreover, we can obtain replication-specific measurements of Young's modulus by splitting the data based on replication and repeating the modeling process outlined above. These values are used to examine heritability, environment, and G×E interactions (Section 2.6). Third, we fit the posited regression model for every possible weighting combination described in Ω and identify the optimal weighting combination to be the one that provides the largest coefficient of determination (R^2).

2.6. Machine learning models for prediction of flexural stiffness

To further explore the relationship between intermediate phenotypes and flexural stiffness, we deployed extreme gradient boosting (Xgboost), a common machine learning technique that automatically detects non-linear relationships and higher-order interactions. The 30 intermediate phenotypes available in the 2019 data included major diameter, minor diameter, rind thickness, rind puncture resistance, moment of inertia, section modulus, linear density, and integrated puncture score recorded on three stalk sections (top, middle, and bottom), and lignin, cellulose, and hemicellulose measured on the ear and bottom internodes. Except for lignin, cellulose, and hemicellulose, all other 24 intermediate phenotypes were available in the 2021 dataset. The Xgboost model was trained using the *caret* package in R, with the tuning of the number of

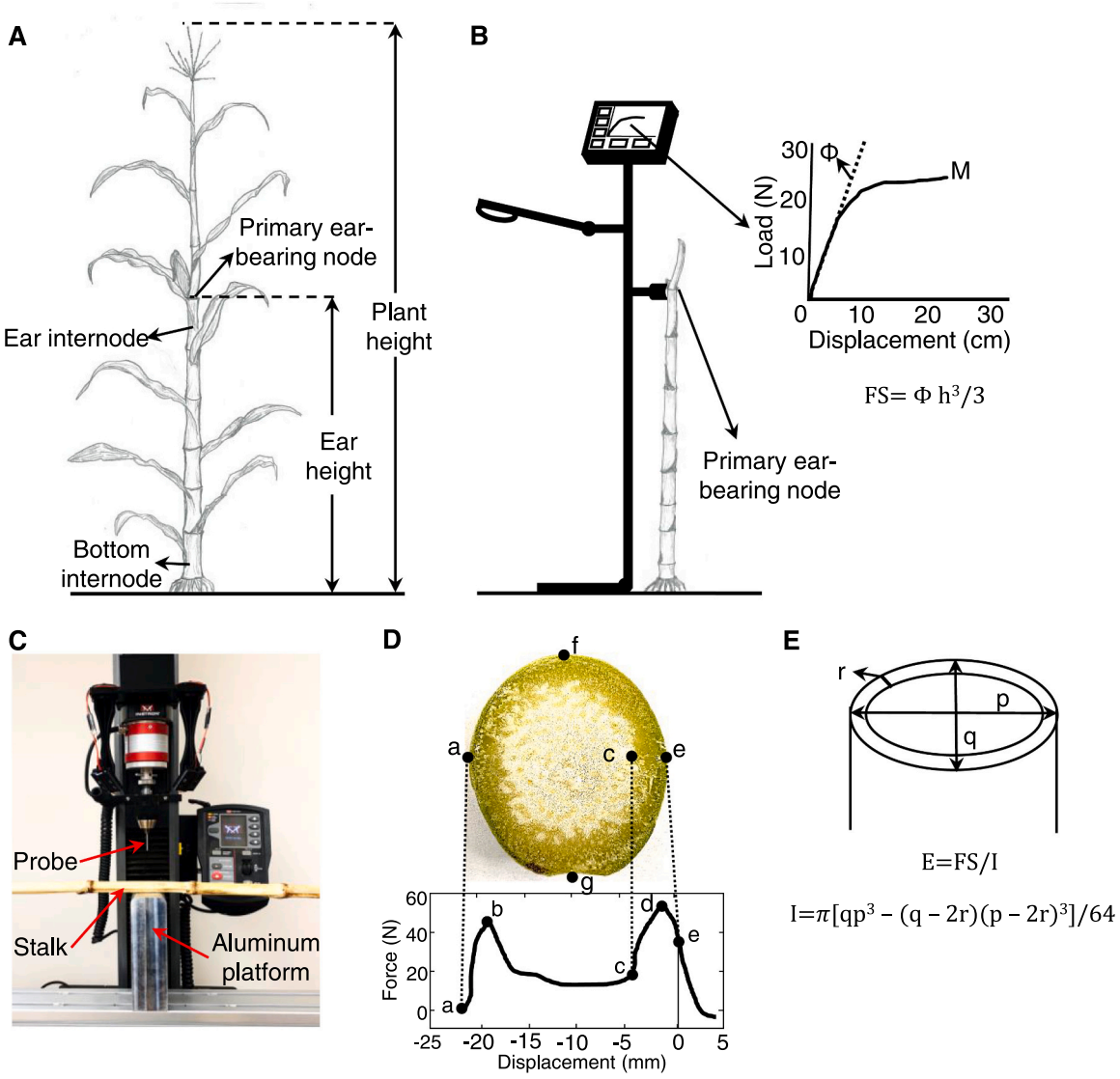

Fig. 2. Phenotyping methodology for recording data on different traits. (A) Diagram of a maize plant showing the naming system of internodes used in the study. (B) Measurement of stalk flexural stiffness with DARLING as discussed in the text. Briefly, Φ is the slope of the linear section of the load-displacement curve, and h is the height set for the DARLING load sensor for pushing the stalk. (C-D) Instron measurements of various stalk properties as described elsewhere (Seegmiller et al., 2020). Briefly, in panel D, the distance from point a to point e represents the minor diameter of the stalk, the larger of points b and d represent rind puncture resistance, the distance from point c to point e is the rind thickness. Note that point e resides at 0 displacement (i.e., the top surface of the aluminum platform shown in panel C). Distance between points f and g is the major diameter of the stalk and was measured with Vernier caliper. (E) A diagram of the stalk cross section showing the calculation of Young's modulus (E) from the moment of inertia (I) and flexural stiffness (FS). The line segments p and q represent major and minor diameters, respectively, and r indicates rind thickness.

trees and interaction depth being guided by 10-fold repeated cross-validation repeated ten times. To detect potential overfitting in implementing the Xgboost model, a holdout set consisting of 20 % of the data was retained as a test set, i.e., the model was not trained on these data, and this data provides a venue to assess the out-of-sample prediction performance.

2.7. Statistical analyses

To detect the effects of hybrid and environment on the phenotype expression of a given trait, the following statistical model was developed:

$$Y_{ijk} = \mu + \alpha_i + \beta_j + \lambda_k + \gamma_{ij} + \varepsilon_{ijk}$$

Where Y_{ijk} denotes the overall phenotype value for a given trait, μ is the grand mean, α_i is the genotype (hybrid) effect, β_j is the effect of the environment (year), λ_k is the random effect of replication nested within the environment, γ_{ij} is the effect of G×E interaction, and ε_{ijk} is the random error. The model terms were estimated using Least Squares and then tested using ANOVA techniques. If model terms were found to be significant, genotype and environment means were compared using Fisher's protected least significant difference test. Test p-values less than $\alpha = 0.05$ were considered evidence of statistical significance. All statistical calculations for comparing genotypes and environments were performed using JMP Pro (version 16.0.0; SAS Institute Inc., Cary, NC).

To estimate the genotypic and phenotypic variances necessary for estimating heritability, the following statistical model was developed:

$$Y_{ij} = \mu + \alpha_i + \beta_j + \gamma_{ij} + \varepsilon_{ij}$$

Where Y_{ij} denotes the overall phenotype value for a given trait, μ is the grand mean, α_i is the random genotype effect, β_j is the random effect of the environment (a combination of replication and environment), γ_{ij} is

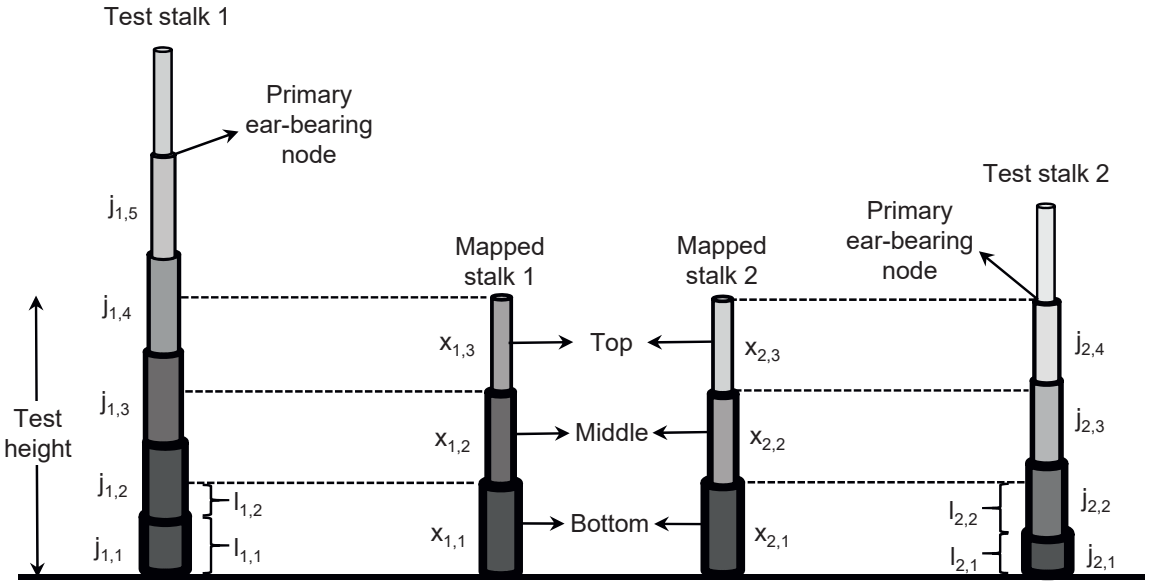

Fig. 3. Schematic diagram of the methodology for generating mapped sections of the stalks using actual phenotype data. Stalks 1 and 2 represent two sibling plants of the same maize hybrid. Phenotypic values on individual internodes on stalks 1 and 2 are labeled $j_{1,1}$ to $j_{1,5}$ and $j_{2,1}$ to $j_{2,4}$, respectively, starting from the bottom internode to the ear internode. Similarly, $x_{1,1}$ to $x_{1,3}$ and $x_{2,1}$ to $x_{2,3}$ represent the mapped sections of stalks 1 and 2, respectively. Lengths of different internodes and internode segments on stalks 1 and 2 accounting for the bottom sections ($x_{1,1}$ and $x_{2,1}$) of the concerned mapped stalks are indicated by $l_{1,1}$ and $l_{1,2}$ and $l_{2,1}$ and $l_{2,2}$, respectively. The dashed lines indicate the boundaries of different sections on mapped stalks and are used as reference points to map the phenotype data from actual stalks. Weighted values of intermediate phenotypes for different sections of the mapped stalks are obtained as given in the example below for the bottom sections: $x_{1,1} = [(j_{1,1}*l_{1,1}) + (j_{1,2}*l_{1,2})]/(l_{1,1} + l_{1,2})$, $x_{2,1} = [(j_{2,1}*l_{2,1}) + (j_{2,2}*l_{2,2})]/(l_{2,1} + l_{2,2})$.

the random effect of G×E interaction, and ε_{ij} is the random error. The variance components associated with the model terms were estimated using Restricted Maximum Likelihood.

Broad sense heritability (Johnson et al., 1955) was estimated as:

Heritability

$$(H^2) = \frac{\sigma_g^2}{\sigma_p^2}$$

where $\sigma_p^2 = \sigma_g^2 + \sigma_e^2 + \sigma_{ge}^2 + \sigma_\varepsilon^2$. and σ_p^2, σ_g^2, σ_e^2, σ_{ge}^2, and σ_ε^2 denote estimates of the phenotypic, genotypic, environmental, G×E interaction, and error variances, respectively. All statistical calculations for heritability estimation were performed using JMP Pro (version 16.0.0; SAS Institute Inc., Cary, NC).

To calculate the Pearson correlation coefficients (Rodgers and Nicewander, 1988) for determining the association between traits, the *corrplot* package in R (Wei and Simko, 2021) was used. Other analyses and figures were made using R Statistical Software (version 4.2.1; R Core Team 2021).

3. Results

3.1. Standardization of phenotyping methodologies

The lack of standard phenotyping protocols poses a major difficulty in understanding the genetic determinants of stalk lodging resistance. In the current study, we implemented a field-based phenotyping approach for measuring morphological (organ geometry and plant shape) and structural traits associated with stalk lodging resistance (Fig. 2; Table 2). We also implemented lab-based approaches to measure the geometric properties of the stalks based on new and published methods (see Seegmiller et al., 2020). This methodology will facilitate systematic data collection on various stalk phenotypes with reduced experimental error.

3.2. Phenotypic variation for stalk flexural stiffness and intermediate phenotypes

The ten inbred lines used for developing hybrids evaluated in the study are genetically diverse and represent diverse heterotic groups (Table 1). The resulting hybrids exhibited a wide and statistically significant variation for stalk flexural stiffness ($P < 0.001$) ranging between 17.19 Nm^2 to 65.02 Nm^2 with a mean of 33.89 Nm^2 and a median of 31.05 Nm^2 (Fig. 4). The effect of environment on stalk flexural stiffness was also found to be significant ($P < 0.05$) between the two environments. Remarkably, certain hybrids showed a broader range of variation within and across the two environments (e.g., PHPR5/Mo17 and PHG35/B73), while others showed negligible variation (e.g., CH701–30/Mo17 and Mo45/Mo17). Furthermore, such variation within and across environments was higher for the hybrids with higher flexural stiffness. Interestingly, the hybrids generated by B73, an inbred line belonging to the Iowa Stiff-Stalk Synthetic heterotic group, had generally higher flexural stiffness compared to those generated by Mo17 inbred belonging to the non-Iowa Stiff-Stalk Synthetic group. To test if the B73 hybrids were stronger than the Mo17 hybrids, we performed linear contrast to compare averages. The results indicated statistically significant differences ($P < 0.001$) between the two groups of hybrids.

To assess the relative contribution of geometric traits and material properties to flexural stiffness, we computed and compared variations in the moment of inertia and Young's modulus of stalks. Variation in the moment of inertia (Section 2.6) was found to be statistically significant among the hybrids ($P < 0.001$) and across environments ($P < 0.05$), indicating the role of both genetic and environmental effects in determining the geometric properties. Remarkably, the average values of the moment of inertia and the magnitude of variation among hybrids were consistently higher in 2021 compared to 2019, suggesting a higher impact of G×E interaction on the trait. Certain hybrids (e.g., PHZ51/B73, A680/Mo17) exhibited statistically significant variation in the moment of inertia between environments compared to others (e.g., CH701–30/Mo17, N7A/B73). Noticeably, the moment of inertia values for all hybrids derived from certain female parents (e.g., A680, PHZ51)

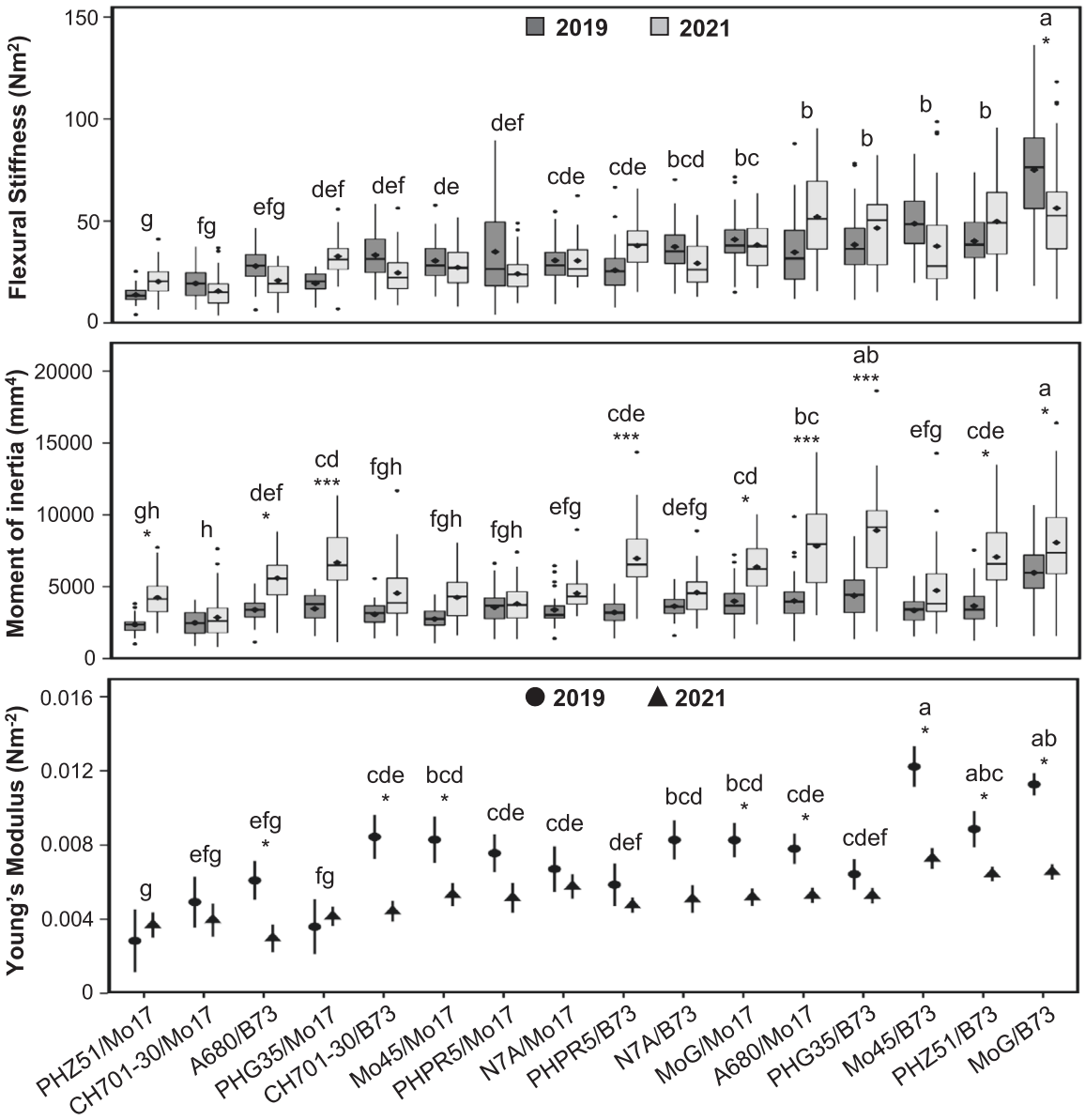

Fig. 4. Comparison of variation in stalk lodging resistance with that of geometric and material properties of stalks. Boxplots are shown in the top and middle panels due to the availability of single plant data for flexural stiffness and moment of inertia from both environments for each hybrid listed on the x-axis. For each boxplot, solid diamonds and horizontal lines indicate the mean and median, respectively, and the outliers are shown by dots at the ends of the whiskers. In the bottom panel, the shapes represent the mean estimates of Young's modulus for each hybrid, and the bars indicate 95 % confidence intervals. The means were compared using Fisher's protected least significant difference test and hybrids marked with different letters denote significant differences ($\alpha = 0.05$). One, two, and three asterisks indicate significant differences between the environments at $P < 0.05$, 0.01, and 0.001, respectively.

were significantly different between environments, whereas such statistical differences were not observed for hybrids of some of the other female parents (e.g., CH701–30, N7A, Mo45) highlighting the genetic component of G×E interaction of this trait. Young's modulus of individual hybrids, the average value represented by the estimate and 95 % confidence intervals and calculated using the regression model described in 2.6, also showed broad and statistically significant variation among the hybrids (Fig. 4). Remarkably, the variation for Young's modulus in the two environments was significant for certain hybrids (e.g., Mo45/B73, PHZ51/B73) and statistically unsubstantial for others (e.g., CH701–30/Mo17, N7A/Mo17). Furthermore, a comparison of the relative phenotypic values of Young's modulus and flexural stiffness in the two environments revealed that the two traits showed the same trend for certain hybrids (e.g., CH701–30/B73, Mo45/B73) whereas the trend was reversed for others (e.g., PHZ51/B73, A680/Mo17). These observations underscore the existence of genetic variation and variable levels of G×E interaction for two important stalk-level traits and indicate that geometric and material properties are important determinants of stalk lodging resistance.

To examine the impact of geometric and structural properties of individual internodes on stalk strength, we recorded key internode-level phenotypes deemed to be associated with stalk lodging resistance. The number of internodes in different hybrids showed significant variation ($P < 0.001$) and ranged from 4 to 8 among different hybrids (Fig. 5). Likewise, we noticed substantial variation for various traits measured on individual internodes in both environments that included internode length, moment of inertia, section modulus, and linear density (Fig. 6; Supplementary Fig. A2-A3). Furthermore, all internode traits also

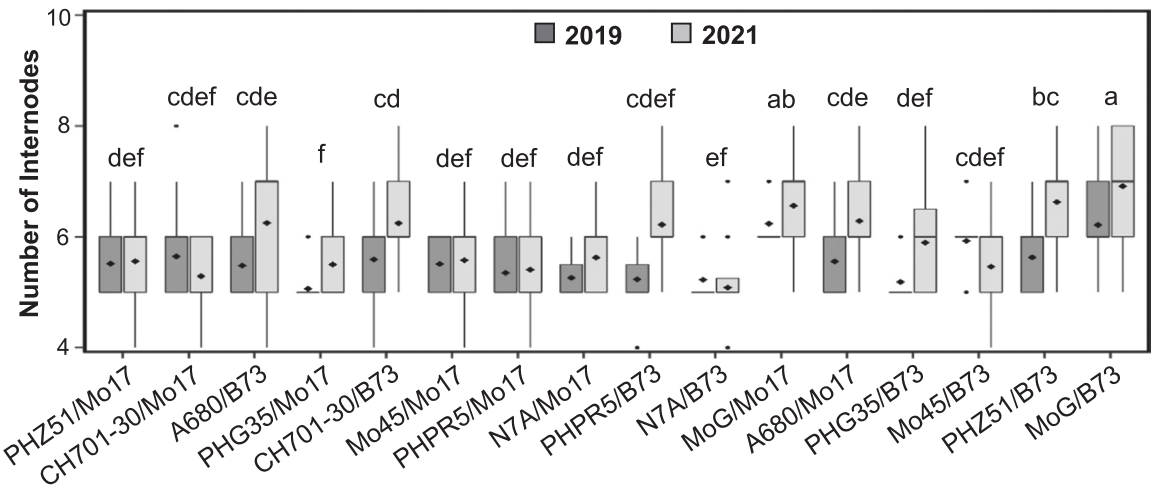

Fig. 5. Variation in the number of elongated internodes on the stalk below the primary ear-bearing node. For each boxplot, solid diamonds and horizontal lines indicate the mean and median, respectively, and the outliers are shown by dots at the ends of the whiskers. Hybrids marked with different letters denote significant differences ($\alpha = 0.05$).

showed substantial intra-plot variation, indicating an important role of the microenvironment in specifying these traits. Moving up from the bottom to the ear internode, we observed a gradual shift in phenotypic values for different traits (Fig. 6). A comparison of bottom and ear internodes revealed statistically significant differences for the intermediate phenotypes. Except for internode length, phenotypic values for all the intermediate phenotypes were consistently higher in magnitude for the bottom internode in all hybrids.

To ask if variation in geometric and structural properties is reflected in chemical composition, we compared insoluble sugars (cellulose and hemicellulose) and lignin content in the bottom and ear internodes (Fig. 7). While hemicellulose was consistently higher in the ear internode, cellulose contents showed genotype-specific patterns where certain hybrids (e.g., CH701–30/Mo17, Mo45/Mo17) had higher cellulose in the ear internode and others (A680/B73, PHG35/Mo17) had higher cellulose in bottom internode. Lignin followed an opposite trend to hemicellulose, as the bottom internodes had consistently higher lignin deposition than the ear internodes in all hybrids.

3.3. Genetic variation and heritability

Significant genetic variance was observed for most traits, both for individual environments and in the combined analysis for both environments, indicating a strong underlying genetic component (Table 3). Internode length, rind thickness, and rind puncture resistance of the bottom internode were the only traits with a nonsignificant genetic variance in the combined analysis of two environments, indicating a substantial environmental impact on these phenotypes. Broad sense heritability estimates followed a similar trend and varied for traits and environments, implying a significant role of genetic and environmental components in the inheritance of these traits. Among the traits measured at the stalk level, flexural stiffness and moment of inertia were more impacted by G×E interaction compared to Young's modulus, as evident from the fluctuation in heritability estimates in the two environments. Intermediate phenotypes measured on the ear internode generally had higher heritability than those measured on the bottom internode. Following a proposed classification (Robinson et al., 1949), flexural stiffness of the stalk, and minor diameter and section modulus of ear internode had higher (>60 %) heritability, while most traits had moderate (30–60 %) heritability. Finally, except for flexural stiffness, all traits had highly significant G×E interaction variance components, indicating the role of the environment in modulating the manifestation of these traits. These findings provide useful entry points for identifying genetically tractable intermediate phenotypes to be targeted for resolving the genetic architecture of stalk lodging resistance.

3.4. Association between stalk flexural stiffness and intermediate phenotypes

To assess the estimated contribution of intermediate phenotypes of individual internodes to stalk lodging resistance, we examined the correlation of the traits with flexural stiffness. Since flexural stiffness was based on test height that varied among hybrids, the number of internodes contributing to the measurement also varied. Given such variation, the four basal internodes that contributed to flexural stiffness measurements on all hybrids in both environments were used for the analysis. All geometric and structural traits recorded on individual internodes, except for internode length, were significantly ($P < 0.001$) and positively correlated with flexural stiffness in both environments (Fig. 8; Table 4; Supplementary Fig. A4-A6; Supplementary Table B2). Among the material traits, lignin and hemicellulose showed significantly negative correlations ($P < 0.001$ and $P < 0.01$, respectively) for the bottom internode in one environment. To summarize, the intermediate phenotypes measured in the study appear to positively impact stalk lodging resistance.

3.5. Prediction of stalk lodging resistance using intermediate phenotypes

To ask which intermediate phenotypes have a sizeable impact on stalk lodging resistance, we modeled flexural stiffness based on intermediate phenotypes by employing engineering-informed and machine learning models. Based on structural engineering beam theory, the engineering-informed model only used three geometric traits (i.e., major diameter, minor diameter, and rind thickness) and achieved an $R^2 = 0.74$ and 0.80, and root mean square error (RMSE) = 9.72 and 8.11 for 2019 and 2021 data, respectively. The machine learning model also demonstrated high predictive performance. For 2019, the correlation (r) between the observed and predicted flexural stiffness for the test and training sets were 0.79 and 0.96, and RMSE for the test and training sets were 10.44 and 5.76, respectively. Likewise, for 2021, we achieved correlations of 0.76 and 0.89 and RMSE of 11.83 and 8.32 for the test and training sets, respectively. A comparison of variable importance score of all internode traits measured in 2019, computed based on the machine meaning model, indicated that the major diameter and moment of inertia of the middle stalk section and lignin content of the bottom internode are the three most important predictors of stalk flexural stiffness (Fig. 9). For 2021, major diameter, moment of inertia, and section modulus of the bottom stalk section were the top three important

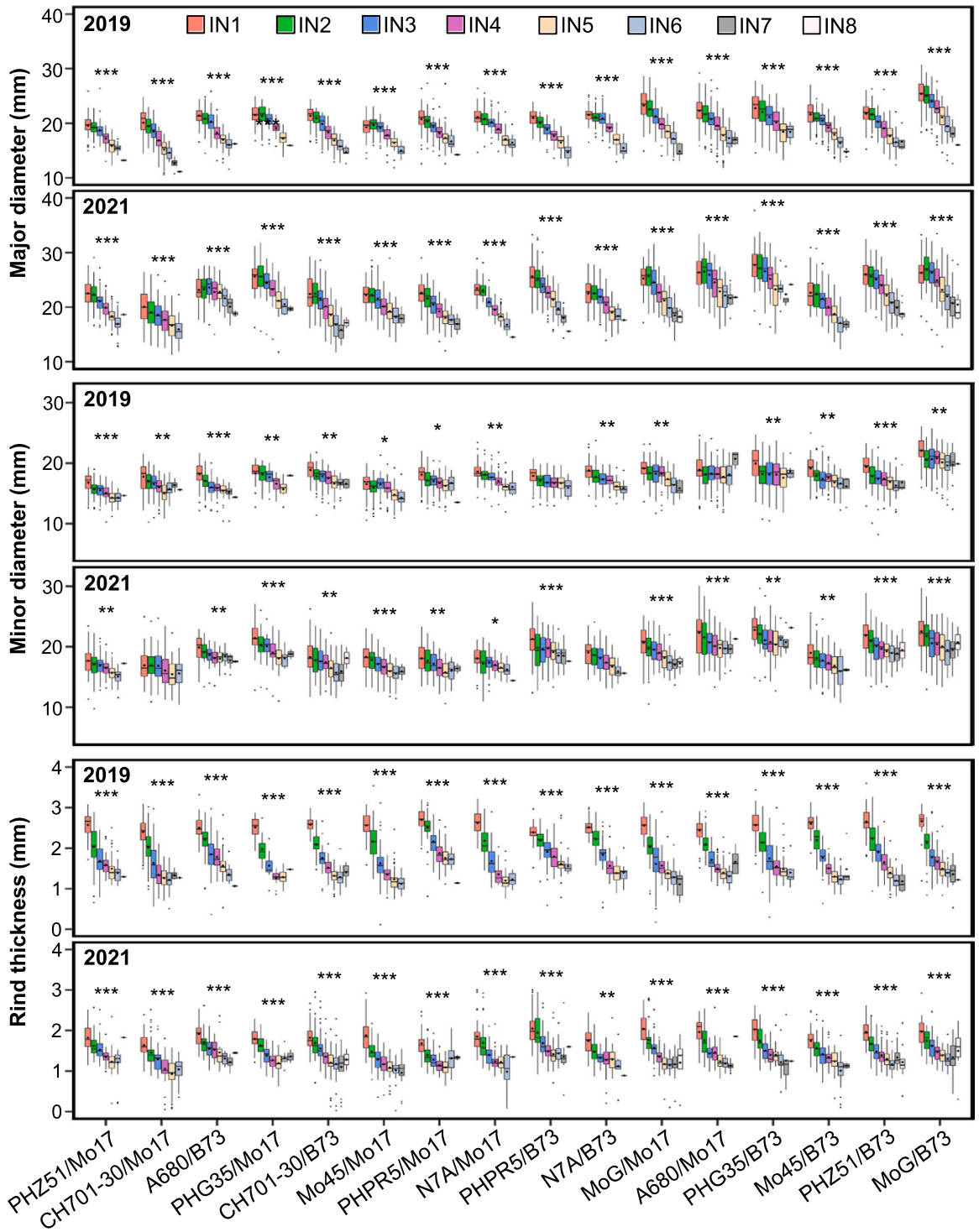

Fig. 6. Variation in geometric properties of elongated internodes on the stalk section below the primary ear-bearing node. For each boxplot, solid diamonds and horizontal lines indicate the mean and median, respectively, and the outliers are shown by dots at the ends of the whiskers. IN1 to IN8 represent contiguous internodes labeled bottom-up starting from the bottom internode. One, two, and three asterisks indicate significant differences between bottom and ear internodes at $P < 0.05$, 0.01, and 0.001, respectively.

predictors of stalk flexural stiffness. The discrepancies in results between the two environments, in terms of the variable importance score for different intermediate phenotypes identified by the machine learning model, are expected and can be explained by the high degree of multicollinearity among the intermediate phenotypes. In summary, marginal statistical models based on three geometric traits effectively predict flexural stiffness, indicating the utility of these traits in artificial selection for stalk lodging resistance.

In comparing the performance of the engineering-informed model to that of the machine learning model, the engineering-informed model is explainable and aptly identifies intermediate phenotypes that could be used to improve stalk lodging resistance via indirect selection for such traits. Though adept at prediction, the machine learning model cannot do the same despite the additional advantage of leveraging a more extensive set of intermediate phenotypes compared to the engineering-informed model.

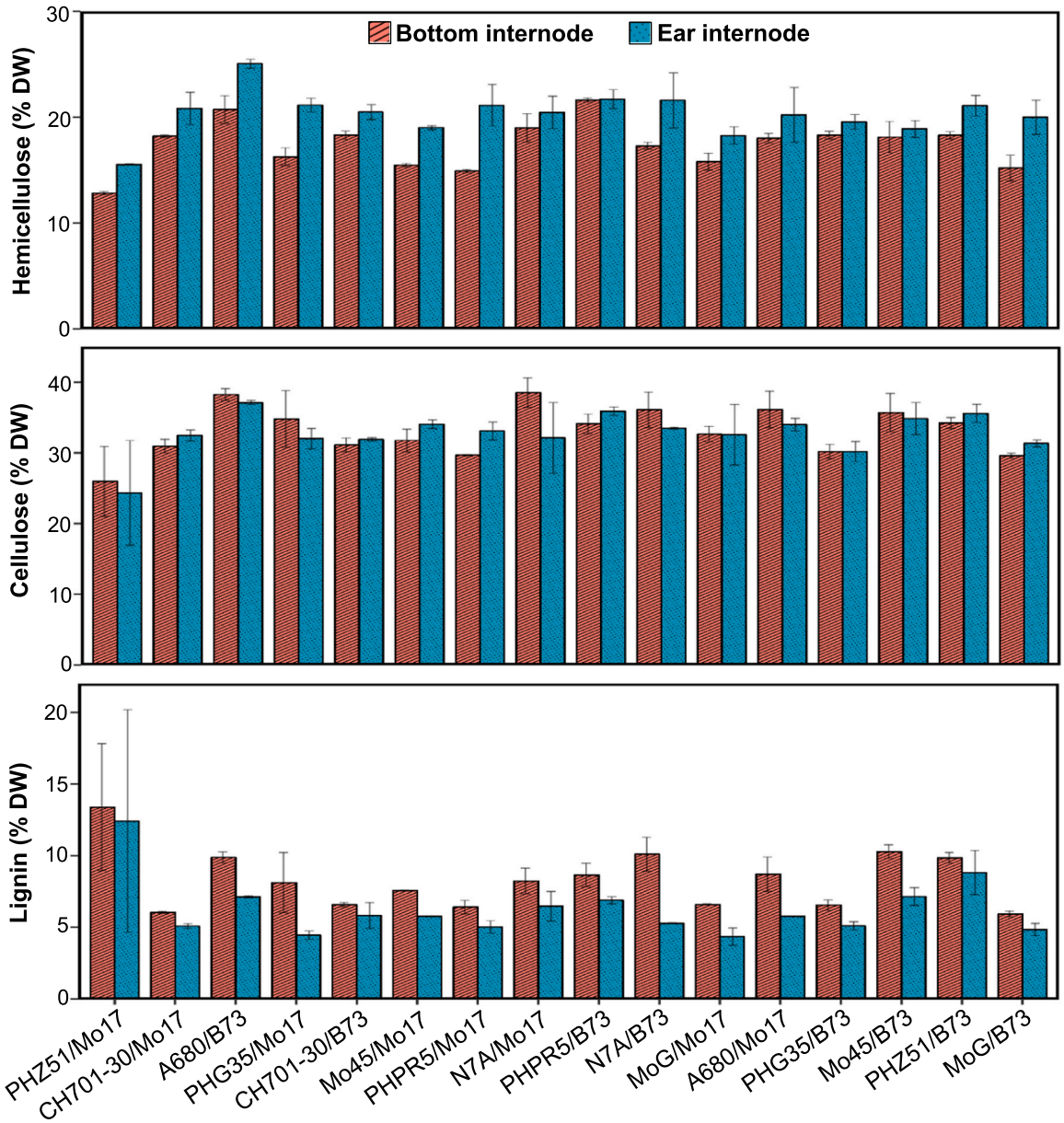

Fig. 7. Variation in material properties of the bottom and ear internodes of the stalks phenotyped in 2019. The error bars are the standard error of the mean based on two replications. DW, Dry matter weight.

4. Discussion

One of the major hindrances in the genetic improvement of stalk lodging resistance is the lack of effective, uniform, replicable, and user-independent phenotyping methods. Flexural stiffness is a reliable indicator of stalk bending strength and, therefore, stalk lodging resistance (Cook et al., 2019; Sekhon et al., 2020). For example, previous studies have shown linear R^2 values between flexural stiffness and bending strength in the range of 0.8 (Robertson et al., 2016). Flexural stiffness can be measured nondestructively, on a plant-by-plant basis, and provides a continuous (not binary) and absolute (not relative) predictor of lodging resistance (Cook et al., 2019; Erndwein et al., 2020). Conversely, natural lodging counts are binary (lodged vs. not lodged) and only provide relative rankings of lodging propensity at the plot level (DeKold and Robertson, 2023). A key advantage of biomechanical phenotyping is that measurements can be acquired in the absence of natural lodging. In addition, flexural stiffness measurements have been shown to be predictive of historical lodging rates gathered in much more extensive and expensive multi-year or multi-location studies (Sekhon et al., 2020). Flexural stiffness demonstrated a significant genetic variance component and high (>60 %) overall heritability across the two environments in the study, supporting the use of this phenotype in genetic and breeding studies. However, substantial fluctuation of the heritability estimates across the two environments in this study indicates a significant contribution of G×E interaction in specifying flexural stiffness and highlights the importance of identifying intermediate phenotypes with high and stable heritability across environments.

4.1. Flexural stiffness and intermediate phenotypes are genetically tractable and impacted by the environment

High heritability for flexural stiffness demonstrates the genetic tractability of this complex phenotype and underscores the importance of the phenotype for germplasm improvement in breeding programs.

Table 3
Variance components and heritability for different traits.

#	Trait	2019		2021		Combined			
		V_G	H^2	V_G	H^2	V_G	V_E	V_{GE}	H^2
1	Flexural stiffness (stalk)	**	0.85	*	0.45	**	NS	**	0.64
2	Young's modulus (stalk)	**	0.51	**	0.55	**	NS	****	0.29
3	Moment of inertia (stalk)	**	0.85	*	0.58	**	NS	****	0.30
4	Length (bottom internode)	NS	0.30	NS	0.19	NS	NS	****	0.00
5	Length (ear internode)	**	0.86	*	0.51	**	NS	****	0.39
6	Major diameter (bottom internode)	**	0.81	NS	0.56	**	NS	****	0.37
7	Major diameter (ear internode)	**	0.73	***	0.43	**	NS	****	0.40
8	Minor diameter (bottom internode)	**	0.82	**	0.59	**	NS	****	0.47
9	Minor diameter (ear internode)	**	0.83	*	0.67	**	NS	****	0.64
10	Rind thickness (bottom internode)	NS	0.14	NS	0.12	NS	NS	****	0.00
11	Rind thickness (ear internode)	**	0.61	*	0.64	**	NS	****	0.29
12	Rind puncture resistance (bottom internode)	NS	0.33	NS	0.19	NS	NS	****	0.16
13	Rind puncture resistance (ear internode)	**	0.81	**	0.75	**	NS	****	0.47
14	Linear density (bottom internode)	**	0.78	***	0.66	*	NS	****	0.48
15	Linear density (ear internode)	**	0.58	**	0.84	**	NS	****	0.53
16	Moment of inertia (bottom internode)	**	0.82	*	0.54	**	NS	****	0.55
17	Moment of inertia (ear internode)	**	0.74	**	0.73	**	NS	****	0.70
18	Section modulus (bottom internode)	**	0.84	*	0.50	**	NS	****	0.53
19	Section modulus (ear internode)	**	0.75	**	0.73	**	NS	****	0.68
20	Integrated puncture score (bottom internode)	**	0.65	*	0.60	**	NS	****	0.47
21	Integrated puncture score (ear internode)	NS	0.24	***	0.45	*	NS	****	0.39

V_G, genetic variance; V_E, environmental variance; V_{GE}, genetic environmental interaction variance; H^2, heritability in the broad sense. One, two, three, and four asterisks indicate statistical significance at $P < 0.1$, 0.05, 0.01, and 0.001; NS, nonsignificant.

Further, the majority of the stalk and internode level intermediate phenotypes had moderate to high heritability, indicating their genetic tractability, as also reported in earlier studies (Liu et al., 2022; Liu et al., 2020). This observation highlights the importance of organ-level resolution in the studies focused on understanding the genetic architecture of these traits and enhancing the mechanistic understanding of stalk lodging resistance. Furthermore, all traits show significant variation across the two environments, indicating an important G×E interaction component of the observed phenotypic variation. Resolving the extent and sources of variation of these traits and their relative contribution to stalk strength on diverse germplasm will further refine the heritability estimates and boost efforts toward the genetic improvement of stalk lodging resistance. It should be noted that the current study is based on two environments, and evaluating more genotypes in diverse environments will be needed to better understand the genetic and environmental underpinnings of these traits. A detailed outline of the phenotyping methodologies for evaluating various intermediate phenotypes will be valuable in generating and sharing uniform datasets across research groups.

4.2. Material and geometric properties collectively determine stalk lodging resistance

Based on structural engineering beam theory, the strength of the stalk is determined by a combination of geometric and material properties, albeit the relative contribution of these two parameters remains largely unknown. Furthermore, while the geometric and material properties are expected to vary across internodes, such differences are often unaccounted for as the majority of the empirical studies usually rely on single-point measurements on stalks (Stubbs et al., 2022a; Xue et al., 2020; Zhang et al., 2021). Highly significant genetic variation among hybrids for the moment of inertia and Young's modulus across the stalks indicate that these parameters are genetically controlled. Remarkably, the lower phenotypic value of one of these two parameters is complemented by a higher phenotypic value for the other parameter, such that the overall flexural stiffness remains unchanged (Fig. 3). This observation allowed us to refine previous reports, which were primarily focused on the geometric properties of stalks and which suggested geometric properties may consistently outweigh material properties in determining structural properties like flexural stiffness (Forell et al., 2015; Stubbs et al., 2022a). Consequently, depending upon the breeding objective (i.e., grain or forage yield), breeding efforts can be focused on either material or geometric properties to get the desired combination while maintaining high stalk lodging resistance. For example, when breeding for increased grain yield under high planting density, improving material properties can compensate for weaknesses in stalk geometric properties induced by decreased stalk diameter (Forell et al., 2015).

4.3. Phenotyping individual internodes is important for understanding the genetic architecture of flexural stiffness

Examination of the role of individual internodes identified various internode properties that determine stalk lodging resistance (Xie et al., 2022; Zhang et al., 2021). However, by focusing on one or a few internodes, such studies do not account for variation in the traits among internodes and the role of such variation in determining overall stalk strength. Significant intra- and inter-plot variation for internode number and length, and for various geometric properties of the individual internodes, including major diameter, minor diameter, and rind thickness, revealed that, besides genetics, the microenvironment is an important determinant of these traits. This prevalent variation has an important bearing on designing breeding studies for the improvement of stalk lodging resistance based on stalk biomechanics. We have previously shown that the maize stalks are not optimally tapered and that uniform taper of stalks was associated with higher flexural stiffness (Stubbs et al., 2020c). This finding shows the importance of understanding the variation in major diameter, minor diameter, and rind thickness, which are the key determinants of the moment of inertia along the length of the stalk. Systematic studies aimed at understanding the specific genetic and environmental regulators of traits of individual internodes are needed to fully characterize the genetic architecture of stalk lodging resistance and

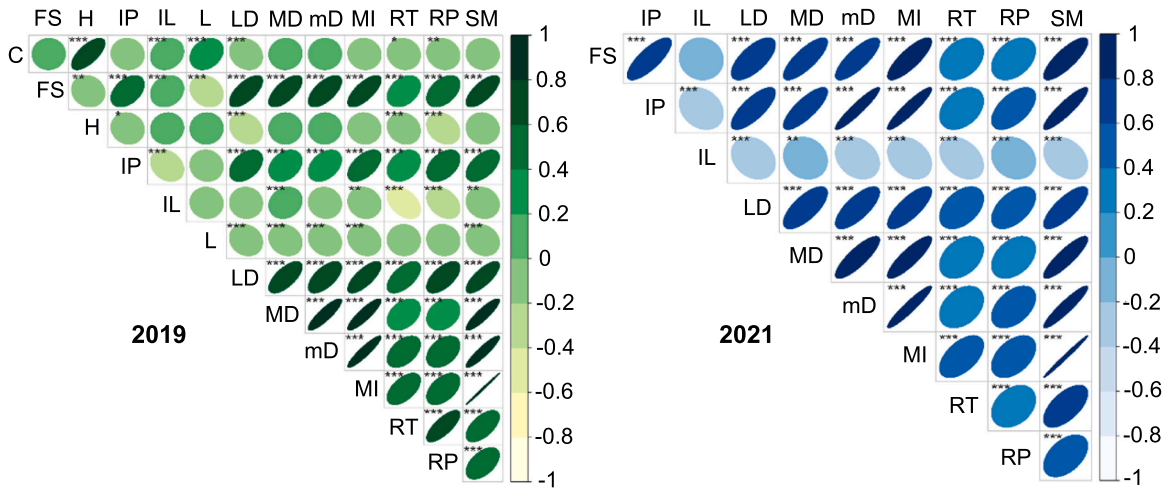

Fig. 8. Correlations of stalk flexural stiffness with intermediate phenotypes recorded on the bottom internode in two environments. One, two, and three asterisks indicate the significance of correlation at $P < 0.05$, 0.01, and 0.001, respectively. C, Cellulose; FS, Flexural stiffness; H, Hemicellulose; IP, Integrated puncture score; IL, Internode length; L, Lignin; LD, Linear density; MD, Major diameter; mD, Minor diameter; MI, Moment of inertia; RT, Rind thickness; RP, Rind puncture resistance; SM, Section modulus.

Table 4
Correlation of intermediate phenotypes with stalk flexural stiffness.

Trait	Stalk flexural stiffness							
Internode	IN1		IN2		IN3		IN4	
Environment	2019	2021	2019	2021	2019	2021	2019	2021
I. Geometric								
Internode length	0.18***	-0.06^{NS}	0.15***	-0.13**	0.07^{NS}	-0.15***	0.05^{NS}	-0.22***
Major diameter	0.67***	0.79***	0.73***	0.79***	0.70***	0.78***	0.74***	0.77***
Minor diameter	0.64***	0.80***	0.59***	0.72***	0.66***	0.73***	0.75***	0.79***
Rind thickness	0.35***	0.33***	0.24***	0.32***	0.23***	0.33***	0.23***	0.36***
Linear density	0.67***	0.67***	0.66***	0.73***	0.57***	0.74***	0.61***	0.72***
Moment of inertia	0.71***	0.82***	0.75***	0.78***	0.75***	0.79***	0.77***	0.79***
Section modulus	0.71***	0.81***	0.74***	0.78***	0.72***	0.78***	0.74***	0.76***
II. Structural								
Rind puncture resistance	0.44***	0.38***	0.36***	0.35***	0.24***	0.37***	0.27***	0.44***
Integrated puncture score	0.43***	0.78***	0.20***	0.71***	0.31***	0.71***	0.32***	0.77***
III. Material								
Cellulose	0.01^{NS}	NA	NA	NA	NA	NA	NA	NA
Hemicellulose	-0.12**	NA	NA	NA	NA	NA	NA	NA
Lignin	-0.20***	NA	NA	NA	NA	NA	NA	NA

One, two, and three asterisks indicate significant differences between the two environments at $P < 0.05$, 0.01, and 0.001, NS, nonsignificant; NA, data not available; IN1, internode 1; IN2, internode 2; IN3, internode 3; IN4, internode 4.

to generate mechanistic understanding. Phenotyping of individual internodes is not practical in most breeding studies and the determination of flexural stiffness with the DARLING will be a more efficient approach to achieving lodging resistance. However, more specialized breeding objectives (e.g., selecting lodging resistance plants with higher stalk biomass) may require selection for individual internode phenotypes. Furthermore, fundamental studies aimed to resolve the biological underpinnings of stalk properties will also require evaluating internode-level phenotypes. Improved higher throughput phenotyping methodologies are needed to alleviate the economic burden of such studies with goals of increased specificity.

4.4. Accounting for trait relationships enhances prediction efficiency for stalk lodging resistance

The marginal model based on structural engineering beam theory that only considered the moment of inertia (I) determined by three geometric traits (major diameter, minor diameter, and rind thickness) was highly effective and explained 74–80 % of the phenotypic variation in flexural stiffness. Therefore, the characterization of the genetic architecture of these three traits needs to be prioritized to understand the biological underpinnings of flexural stiffness. The remaining 20–26 % of the variation in flexural can be attributed to Young's modulus (E) and, to a lesser extent, to the inaccuracies in the calculation of the moment of inertia. Expanding the number of intermediate phenotypes and employing a machine learning approach was able to explain a modest (58–62 %) phenotypic variation for flexural stiffness. The superior performance of marginal statistical models over the machine learning approach highlighted the advantage of leveraging the mathematics and physics-based principles for understanding the biological relationships between stalk lodging resistance and its intermediate phenotypes. Machine learning models are based purely on statistics and do not possess inherent logic like engineering-based models. Therefore, machine learning models are unavoidably biased by their training set to a far greater degree than physics-based models. This makes it increasingly difficult to accurately extrapolate their results to other environments or genotypes. We have found that, when available, engineering-based models are often more effective in deciphering lodging resistance and

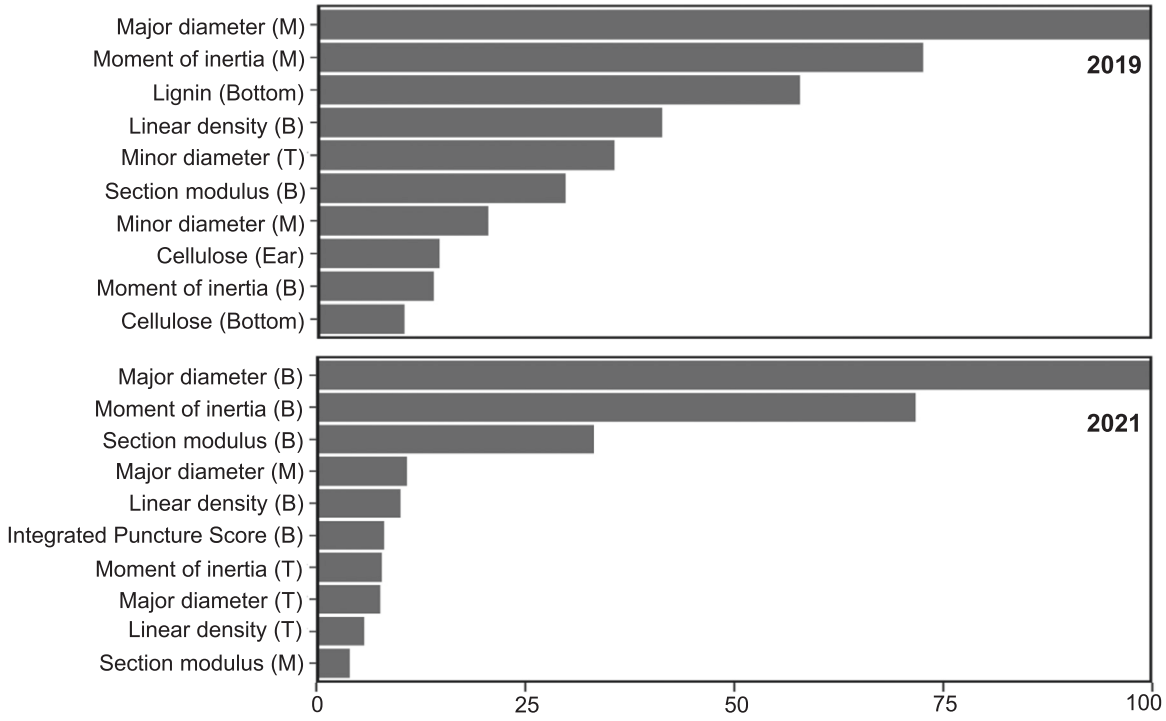

Fig. 9. Identification of important intermediate phenotypes associated with stalk lodging resistance using machine learning modeling. The horizontal bars indicate the variable importance score for different traits measured on a scale of 0–100, as indicated on the x-axis. The top ten most important traits identified are shown on the y-axis; T, M, and B denote the top, middle, and bottom sections of the stalks, whereas Bottom and Ear refer to the bottom and ear internodes as discussed in the text.

generating generalizable principles than machine learning based approaches. Future genetic studies to identify the genes and genetic elements underlying intermediate phenotypes identified through engineering-based models should be prioritized to accelerate the genetic improvement of stalk lodging resistance.

Our current and previous studies highlight the value of changing the experimentation unit from stalk to individual internodes for a comprehensive mechanistic understanding of flexural stiffness (Stubbs et al., 2020c). Furthermore, even less is known about the tissue and cellular level differences that differentiate strong and weak stalks and the genetic underpinnings of such differences. For instance, cell size and shape and differences in cell wall thickness among parenchyma, collenchyma, and sclerenchyma cells influence the moment of inertia of the cells (Dupuy et al., 2010). However, phenotyping of this exhaustive set of the cell- and tissue-level structural, geometric, and material properties is a major challenge, and novel high throughput phenotyping methodologies are needed to fully resolve the regulation of stalk lodging resistance in the future.

5. Conclusions

Standardization of phenotyping protocols and detailed characterization of stalk and internode properties of a small albeit genetically diverse set of hybrids revealed tremendous variation for different intermediate phenotypes underlying stalk lodging resistance. Phenotypic analysis of individual internodes revealed prevalent genetic variation and G×E interaction in controlling the number, length, diameter, linear density, and rind properties of internodes that create a continuum of stalk-level traits. Most of the intermediate phenotypes evaluated in the study showed moderate to high heritability, indicating their genetic tractability for improving stalk lodging resistance. We show that both the geometric and material properties of the stalks are important and complementary determinants of stalk lodging resistance. Marginal statistical models based on structural engineering beam theory showed that 74–80 % variation for flexural stiffness could be explained by accounting for the major diameter, minor diameter, and rind thickness of the stalks. Machine learning models showed lower efficiency than the marginal model by explaining 58–62 % of the variation for flexural stiffness. This study provides a roadmap for breeding efforts to identify superior germplasm and genetic studies to elucidate the genetic architecture of stalk lodging resistance in maize.

CRediT authorship contribution statement

Bharath Kunduru: Methodology, Investigation, Data curation, Formal analysis, Software, Visualization, Writing – original draft, Writing – review & editing. **Rohit Kumar:** Investigation. **Manwinder S. Brar:** Investigation, Writing – review & editing. **Christopher J. Stubbs:** Investigation, Data curation, Formal analysis, Software. **Kaitlin Tabaracci:** Investigation, Data curation, Formal analysis, Software. **Norbert T. Bokros:** Investigation. **William C. Bridges:** Formal analysis, Writing – review & editing. **Douglas D. Cook:** Conceptualization, Methodology; **Seth DeBolt:** Funding acquisition, Writing – review & editing. **Christopher S. McMahan:** Methodology, Data curation, Formal analysis, Software, Visualization, Writing – original draft, Writing – review & editing, Funding acquisition, Supervision. **Daniel J. Robertson:** Conceptualization, Methodology, Investigation, Data curation, Formal analysis, Software, Writing – review & editing, Resources, Project administration, Funding acquisition, Supervision. **Rajandeep S. Sekhon:** Conceptualization, Methodology, Investigation, Data curation, Formal analysis, Writing – original draft, Writing – review & editing, Resources, Project administration, Funding acquisition, Supervision.

Declaration of Competing Interest

The authors declare that they have no known competing financial interests or personal relationships that could have appeared to influence the work reported in this paper.

Data Availability

Data will be made available upon reasonable request to the corresponding author.

Acknowledgments

This work was funded by the National Science Foundation (grant #1826715). The authors acknowledge the generous support from the United States Department of Agriculture - Germplasm Repository Information Network by providing seed germplasm resources. We also thank Abigail Reeves for drawing the pictures of the maize plant and Rebecca Bishop and all the undergraduate students of the KIC consortium for their assistance in data collection. Any opinions, findings, conclusions, or recommendations are those of the author(s) and do not necessarily reflect the view of the funding bodies.

Appendix A. Supporting information

Supplementary data associated with this article can be found in the online version at doi:10.1016/j.fcr.2023.109168.

References

Albrecht, K.A., Martin, M.J., Russel, W.A., Wedin, W.F., Buxton, D.R., 1986. Chemical and in vitro digestible dry matter composition of maize stalks after selection for stalk strength and stalk-rot resistance. Crop Sci. 26, 1051–1055.

Barreiro, R., Carrigan, L., Ghaffarzadeh, M., Goldman, D.M., Hartman, M.E., Johnson, D. L., Steenhoek, L., 2008. Device and method for screening a plant population for wind damage resistance traits. US Patent US 7412880 B2 [Issued on August 19, 2008]. Pioneer Hi-Bred International, Inc., Johnston, IA (US), United States.

Bayer, 2022. Bayer Global - Short Corn is Smart Corn. https://www.youtube.com/watch?v=GbQBDcmdeAw [Accessed on 1 August 2023].

Carter, P.R., Hudelson, K.D., 1988. Influence of simulated wind lodging on corn growth and grain yield. J. Prod. Agric. 1, 295–299.

Cook, D.D., de la Chapelle, W., Lin, T.-C., Lee, S.Y., Sun, W., Robertson, D.J., 2019. DARLING: a device for assessing resistance to lodging in grain crops. Plant Methods 15, 102.

DeKold, J., Robertson, D., 2023. Experimental error analysis of biomechanical phenotyping for stalk lodging resistance in maize. Sci. Rep. 13, 12178.

Dupuy, L., Mackenzie, J., Haseloff, J., 2010. Coordination of plant cell division and expansion in a simple morphogenetic system. Proc. Natl. Acad. Sci. USA 107, 2711–2716.

Durrell, L.W., 1925. A preliminary study of fungus action as the cause of down corn. Phytopathology 15, 146–154.

Elmore, R.W., Ferguson, R.B., 1999. Mid-season stalk breakage in corn: hybrid and environmental factors. J. Prod. Agric. 12, 293–299.

Erndwein, L., Cook, D.D., Robertson, D.J., Sparks, E.E., 2020. Field-based mechanical phenotyping of cereal crops to assess lodging resistance. Appl. Plant Sci. 8, e11382.

FAO, 2022. World Food and Agriculture – Statistical Yearbook 2022. pp. 382. FAO, Rome, Italy.

Flint-Garcia, S.A., Jampatong, C., Darrah, L.L., McMullen, M.D., 2003. Quantitative trait locus analysis of stalk strength in four maize populations. Crop Sci. 43, 13–22.

Forell, G.V., Robertson, D., Lee, S.Y., Cook, D.D., 2015. Preventing lodging in bioenergy crops: a biomechanical analysis of maize stalks suggests a new approach. J. Exp. Bot. 66, 4367–4371.

Foulkes, M.J., Slafer, G.A., Davies, W.J., Berry, P.M., Sylvester-Bradley, R., Martre, P., Calderini, D.F., Griffiths, S., Reynolds, M.P., 2010. Raising yield potential of wheat. III. Optimizing partitioning to grain while maintaining lodging resistance. J. Exp. Bot. 62, 469–486.

Hirsch, C.N., Foerster, J.M., Johnson, J.M., Sekhon, R.S., Muttoni, G., Vaillancourt, B., Peñagaricano, F., Lindquist, E., Pedraza, M.A., Barry, K., de Leon, N., Kaeppler, S.M., Buell, C.R., 2014. Insights into the maize pan-genome and pan-transcriptome. Plant Cell 26, 121–135.

Johnson, H.W., Robinson, H.F., Comstock, R.E., 1955. Estimates of genetic and environmental variability in soybeans1. Agron. J. 47, 314–318.

Josse, J., Husson, F., 2016. missMDA: a package for handling missing values in multivariate data analysis. J. Stat. Softw. 70 (1), 31.

Khobra, R., Sareen, S., Meena, B.K., Kumar, A., Tiwari, V., Singh, G.P., 2019. Exploring the traits for lodging tolerance in wheat genotypes: a review. Physiol. Mol. Biol. Plants 25, 589–600.

Lindsey, A.J., Carter, P.R., Thomison, P.R., 2021. Impact of imposed root lodging on corn growth and yield. Agron. J. 113, 5054–5062.

Liu, H., Wang, H., Shao, C., Han, Y., He, Y., Yin, Z., 2022. Genetic architecture of maize stalk diameter and rind penetrometer resistance in a recombinant inbred line population. Genes 13, 579.

Liu, X., Hu, X., Li, K., Liu, Z., Wu, Y., Wang, H., Huang, C., 2020. Genetic mapping and genomic selection for maize stalk strength. BMC Plant Biol. 20, 196-196.

Loesch, Jr, P.J., Calvert, O.H., Zuber, M.S., 1962. Interrelations of diplodia stalk rot and two morphological traits associated with lodging of corn[1]. Crop Sci. 2, 469–472.

Manga-Robles, A., Santiago, R., Malvar, R.A., Moreno-González, V., Fornalé, S., López, I., Centeno, M.L., Acebes, J.L., Álvarez, J.M., Caparros-Ruiz, D., Encina, A., García-Angulo, P., 2021. Elucidating compositional factors of maize cell walls contributing to stalk strength and lodging resistance. Plant Sci. 307, 110882.

Martin, S.A., Darrah, L.L., Hibbard, B.E., 2004. Divergent selection for rind penetrometer resistance and its effects on european corn borer damage and stalk traits in corn. Crop Sci. 44, 711–717.

Niu, Y., Chen, T., Zhao, C., Zhou, M., 2022. Lodging prevention in cereals: Morphological, biochemical, anatomical traits and their molecular mechanisms, management and breeding strategies. Field Crops Res. 289, 108733.

Rajkumara, S., 2008. Lodging in cereals – a review. Agric. Rev. 29, 55–60.

Robertson, D.J., Smith, S.L., Cook, D.D., 2015. On measuring the bending strength of septate grass stems. Am. J. Bot. 102, 5–11.

Robertson, D.J., Lee, S.Y., Julias, M., Cook, D.D., 2016. Maize stalk lodging: flexural stiffness predicts strength. Crop Sci. 56, 1711–1718.

Robertson, D.J., Julias, M., Lee, S.Y., Cook, D.D., 2017. Maize stalk lodging: morphological determinants of stalk strength. Crop Sci. 57, 926–934.

Robertson, D.J., Brenton, Z.W., Kresovich, S., Cook, D.D., 2022. Maize lodging resistance: stalk architecture is a stronger predictor of stalk bending strength than chemical composition. Biosyst. Eng. 219, 124–134.

Robinson, H.F., Comstock, R.E., Harvey, P.H., 1949. Estimates of heritability and the degree of dominance in Corn1. Agron. J. 41, 353–359.

Rodgers, J.L., Nicewander, W.A., 1988. Thirteen ways to look at the correlation coefficient. Am. Stat. 42, 59–66.

Seegmiller, W.H., Graves, J., Robertson, D.J., 2020. A novel rind puncture technique to measure rind thickness and diameter in plant stalks. Plant Methods 16, 44.

Sekhon, R.S., Joyner, C.N., Ackerman, A.J., McMahan, C.S., Cook, D.D., Robertson, D.J., 2020. Stalk bending strength is strongly associated with maize stalk lodging incidence across multiple environments. Field Crops Res. 249, 107737.

Shah, A.N., Tanveer, M., Abbas, A., Yildirim, M., Shah, A.A., Ahmad, M.I., Wang, Z., Sun, W., Song, Y., 2021. Combating dual challenges in maize under high planting density: stem lodging and kernel abortion. Front. Plant Sci. 12.

Stubbs, C.J., McMahan, C.S., Seegmiller, W., Cook, D.D., Robertson, D.J., 2020a. Integrated Puncture Score: force–displacement weighted rind penetration tests improve stalk lodging resistance estimations in maize. Plant Methods 16, 113.

Stubbs, C.J., Oduntan, Y.A., Keep, T.R., Noble, S.D., Robertson, D.J., 2020b. The effect of plant weight on estimations of stalk lodging resistance. Plant Methods 16, 128.

Stubbs, C.J., Seegmiller, K., McMahan, C., Sekhon, R.S., Robertson, D.J., 2020c. Diverse maize hybrids are structurally inefficient at resisting wind induced bending forces that cause stalk lodging. Plant Methods 16, 67.

Stubbs, C.J., Larson, R., Cook, D.D., 2022a. Maize stalk stiffness and strength are primarily determined by morphological factors. Sci. Rep. 12, 720.

Stubbs, C.J., McMahan, C.S., Tabaracci, K., Kunduru, B., Sekhon, R.S., Robertson, D.J., 2022b. Cross-sectional geometry predicts failure location in maize stalks. Plant Methods 18, 56.

Stubbs, C.J., Kunduru, B., Bokros, N., Verges, V., Porter, J., Cook, D.D., DeBolt, S., McMahan, C., Sekhon, R.S., Robertson, D.J., 2023. Moving toward short stature maize: The effect of plant height on maize stalk lodging resistance. Field Crops Res. 300, 109008.

Thompson, G., Narva, K. , 2009. Corn with transgenic insect protection traits utilized in combination with drought tolerance and/or reduced inputs particularly fertlizer. US Patent Application Publication US 2009/0300980 A1 [Published on 10 December 2009]. Dow AgroSciences LLC, Indianapolis (IN), United States.

USDA, 2021. Grain: World Markets and Trade. https://downloads.usda.library.cornell.edu/usda-esmis/files/zs25×844t/4742b275h/fb495291h/grain.pdf [accessed on 13 February 2023].

Wei, T., Simko, V. , 2021. corrplot: Visualization of a Correlation Matrix.

White, M.R., Mikel, M.A., de Leon, N., Kaeppler, S.M., 2020. Diversity and heterotic patterns in North American proprietary dent maize germplasm. Crop Sci. 60, 100–114.

Xie, L., Wen, D., Wu, C., Zhang, C., 2022. Transcriptome analysis reveals the mechanism of internode development affecting maize stalk strength. BMC Plant Biol. 22, 49.

Xue, J., Ming, B., Xie, R., Wang, K., Hou, P., Li, S., 2020. Evaluation of maize lodging resistance based on the critical wind speed of stalk breaking during the late growth stage. Plant Methods 16, 148.

Ye, D.L., Zhang, Y.S., Al-Kaisi, M.M., Duan, L.S., Zhang, M.C., Li, Z.H., 2016. Ethephon improved stalk strength associated with summer maize adaptations to environments differing in nitrogen availability in the North China Plain. J. Agric. Sci. 154, 960–977.

Zhan, X., Kong, F., Liu, Q., Lan, T., Liu, Y., Xu, J., Ou, Q., Chen, L., Kessel, G., Kempenaar, C., Yuan, J., 2022. Maize basal internode development significantly affects stalk lodging resistance. Field Crops Res. 286, 108611.

Zhang, P., Gu, S., Wang, Y., Yang, R., Yan, Y., Zhang, S., Sheng, D., Cui, T., Huang, S., Wang, P., 2021. Morphological and mechanical variables associated with lodging in maize (Zea mays L.). Field Crops Res. 269, 108178.

Zheng, Z., Guo, B., Dutta, S., Roy, V., Liu, H., Schnable, P.S., 2023. The 2020 derecho revealed limited overlap between maize genes associated with root lodging and root system architecture. Plant Physiol. 192, 2394–2403.

Zuber, M.S., Grogan, C.O., 1961. A new technique for measuring stalk strength in corn. Crop Sci. 1, 378–380.